Organic Semiconductors

DOI: 10.1002/anie.201306668

Dependence of the Properties of Dihydroindenofluorene Derivatives on Positional Isomerism: Influence of the Ring Bridging**

*Maxime Romain, Denis Tondelier, Jean-Charles Vanel, Bernard Geffroy, Olivier Jeannin, Joëlle Rault-Berthelot, Rémi Métivier, and Cyril Poriel**

The future of organic electronics is driven by the synthesis and the study of novel molecular fragments for the construction of highly efficient polymers or oligomers.[1] In this context, poly- and oligophenylene derivatives constitute an important class of highly promising molecules, which have been widely studied for the last two decades.[2,3] Of particular interest in the chemistry and physics of oligophenylenes is the bridged-*para*-terphenyl unit, namely, 6,12-dihydroindeno[1,2-*b*]fluorene (Scheme 1). Although it has been known since the 1950s,[4] investigations of the dihydroindeno[1,2-*b*]fluorenyl core only started a decade ago thanks to the pioneering work of Müllen, which made this molecule a key building block for electronics.[2] There are nowadays numerous examples of efficient dihydroindeno[1,2-*b*]fluorenyl-based semiconductors that have found application in various fields, such as fluorescent[2,3,5–8] and phosphorescent[9] organic light-emitting diodes (OLEDs), organic field-effect transistors,[10–12] and organic solar cells.[13] This wide range of applications clearly shows the high potential of this building block, but also its versatility. However, the dihydroindeno[1,2-*b*]fluorene is not the only member of the bridged-terphenyl family, since it possesses four other positional isomers with different phenyl linkages (*para*/*meta*/*ortho*) and different ring-bridging positions (*anti* vs. *syn*; Scheme 1). There are hence five dihydroindenofluorene positional isomers, each possessing its own ring topology, which in turn has structural and electronic consequences. However, in contrast to the dihydroindeno[1,2-*b*]fluorene, other positional isomers remain very scarce in the literature owing to synthetic difficulties. For example, the dihydroindeno[2,1-*a*]fluorenyl (*syn para*-terphenyl) unit (Scheme 1) has only been investigated for organic electronics very recently,[14] and thanks its particular *syn* geometry has emerged as a promising scaffold for a new generation of excimer-based OLEDs.[15] Similarly, antiaromatic fully conjugated indenofluorene derivatives have recently attracted particular attention;[16–19] Haley and co-workers have for example reported a new class of (2,1-*c*)-indenofluorenes with high electron affinities.[20] However, the *anti* and *syn meta*-terphenyl isomers, that is, dihydroindeno-[1,2-*a*]fluorene and dihydroindeno[2,1-*b*]fluorene, although known for 60 years,[21] are almost absent from the literature,[22] and their intrinsic properties have never been studied.

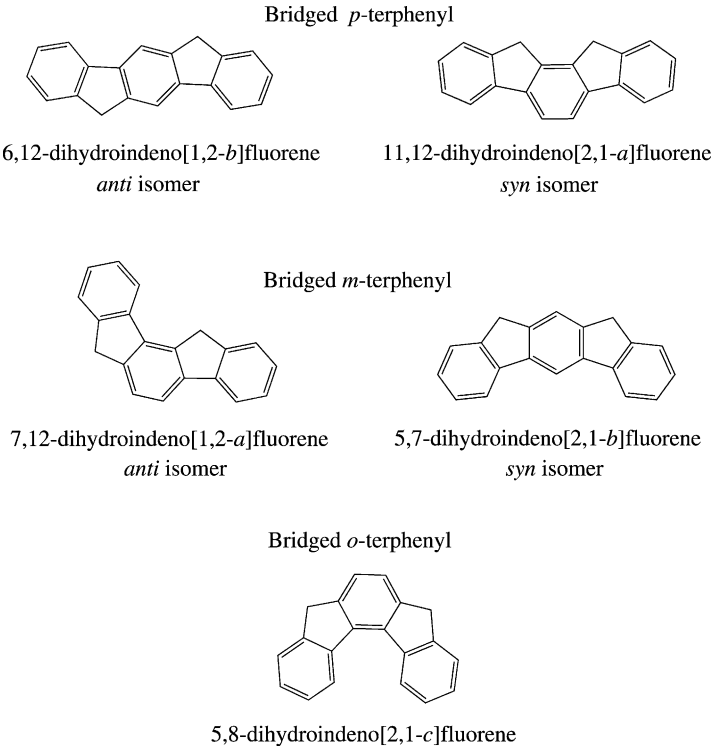

Scheme 1. The five positional dihydroindenofluorene isomers.

As the design of novel molecular fragments is of key importance for the future of organic electronics, we report herein the first examples of the use of dihydroindeno[1,2-*b*]fluorene (**1**) and dihydroindeno[2,1-*a*]fluorene (**2**;

[*] M. Romain, Dr. O. Jeannin, Dr. J. Rault-Berthelot, Dr. C. Poriel
UMR CNRS 6226 "Institut des Sciences Chimiques de Rennes"
Université de Rennes 1
Campus de Beaulieu, 35042 Rennes cedex (France)
E-mail: cyril.poriel@univ-rennes1.fr
Dr. D. Tondelier, J.-C. Vanel, B. Geffroy
UMR CNRS 7647, LPICM, École Polytechnique
91128 Palaiseau (France)
B. Geffroy
LCSI, IRAMIS/SPCSI, CEA Saclay
91191 Gif-sur-Yvette (France)
Dr. R. Métivier
PPSM, Institut d'Alembert, ENS Cachan, UMR CNRS 8531
61 Avenue du Président Wilson, 94235 Cachan (France)

[**] We thank the CDIFX, the CRMPO (Rennes), the CINES (Montpellier), the Region Bretagne, and the ADEME for a studentship (M.R.), and the ANR for financial support (Project HOME-OLED no. ANR-11-BS07-020-01). We also thank Prof. Cornil (Mons) for helpful discussions.

Supporting information for this article is available on the WWW under http://dx.doi.org/10.1002/anie.201306668.

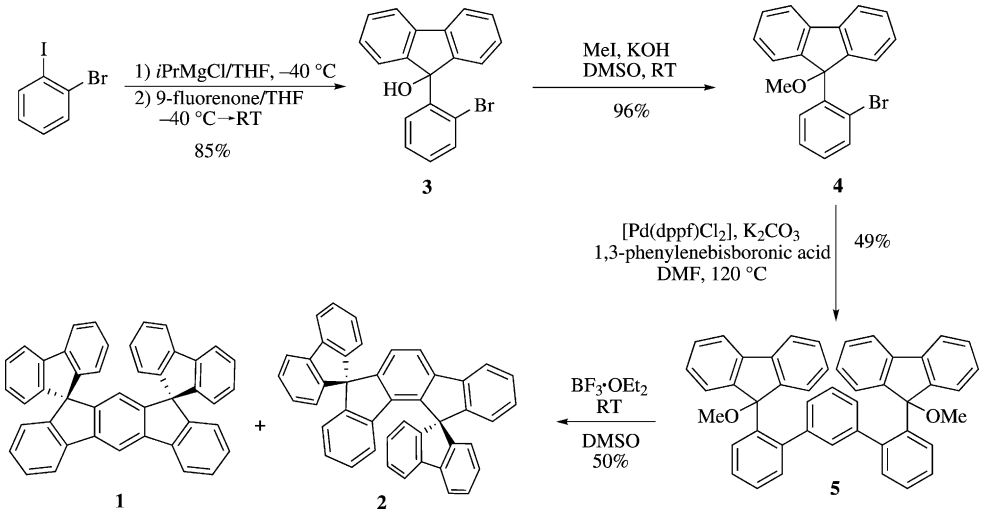

Scheme 2. Synthesis of **1** and **2**. DMF = *N*,*N*-dimethylformamide, DMSO = dimethyl sulfoxide, dppf = 1,1′-bis(diphenylphosphino)ferrocene.

Scheme 2) as the emissive layer (EML) in nondoped blue small-molecule OLEDs (SMOLEDs). Not only does the performance of the devices appear to be around the highest reported for dihydroindenofluorene-based nondoped blue OLEDs, but a remarkable and unusual photophysical feature induced by the ring bridging is also highlighted for the (1,2-*a*) isomer **2**.

The synthetic approach described herein is based on an intramolecular bicyclization reaction, which allows both isomers **1** and **2** to be obtained in the final stage and thus avoids the development of two regioselective routes. The first step of our synthetic investigation (Scheme 2) was to synthesize the fluorenol **3** through a magnesium–iodine exchange reaction on 2-bromo-iodobenzene, followed by the trapping of the intermediate with 9-fluorenone (85%).[23] First attempts to obtain the difluorenol analogue of **5** directly from **3** through a Suzuki–Miyaura cross-coupling reaction failed owing to the formation of a stable palladacycle (see the proposed structure in the Supporting Information). To prevent this side reaction, the hydroxy group of **3** was protected with a methyl group to readily provide the methoxyfluorene derivative **4** (96%). The further cross-coupling of **4** with 1,3-phenylenebisboronic acid provided the key intermediate **5** with the *meta*-terphenyl scaffold in place (49%). The intramolecular electrophilic bicyclization of **5** finally led to the formation of the two isomers dispiro-[fluorene-9,5′-indeno[2,1-*b*]fluorene-7′,9″-fluorene] (**1**) and dispiro[fluorene-9,12′-indeno[1,2-*a*]fluorene-7′,9″-fluorene] (**2**) in a 1:1 ratio. The two isomers were separated by chromatography. This synthetic approach is short (4 steps), efficient, adaptable to other isomers, and allows a gram-scale preparation.

The *syn* and *anti* geometries of **1** and **2** were confirmed by 2D NMR spectroscopic experiments (see the Supporting Information) and by X-ray diffraction on single crystals (Figure 1). The dihydroindeno[1,2-*a*]fluorenyl core of **2** has a maximum length of 10.1 Å and is thus shorter than the dihydroindeno[2,1-*b*]fluorenyl core of **1** (10.6 Å). The maximum length of the bridged *para*-terphenyl homologues also flanked with spirofluorenes, namely, dispiro[fluorene-9,6′-indeno[2,1-*a*]fluorene-12′,9″-fluorene] (**6**) and dispiro[fluorene-9,11′-indeno[1,2-*b*]fluorene-12′,9″-fluorene] (**7**; see structures in the Supporting Information) has been reported at 10.8 and 11.1 Å, respectively.[24] These values clearly indicate a strong contraction of the dihydroindenofluorenyl cores of **1** and **2**. The *meta* linkages of the constituent phenylene rings in the dihydroindeno[1,2-*a*]/[2,1-*b*]fluorenyl cores are partially

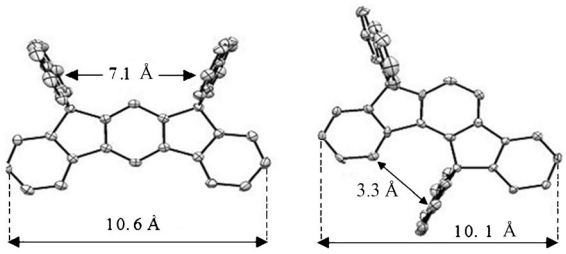

Figure 1. ORTEP drawings of **1** (left) and **2** (right). Ellipsoids are drawn at the 50% probability level, hydrogen atoms have been omitted.

responsible for this contraction. In the case of **2**, the contraction is even further accentuated by the presence of a spiro bridge *ortho* to the two phenyl linkages. In addition, the dihydroindeno[2,1-*b*]fluorenyl core found in **1** is almost flat. Hence, the π-conjugation is maximized in **1**, with dihedral angles between the plane of the central phenyl ring and those of the side rings of approximately 2.5 and 0.5° (see the Supporting Information). The dihydroindeno[1,2-*a*]fluorenyl core of **2** presents more pronounced deformations with dihedral angles of approximately 6.5 and 3.7° owing to the strong contraction imposed by the ring bridging. This ring bridging, which leads to an *anti* geometry, induces a very short distance between the plane of a spirofluorene moiety and the facing phenyl ring of the dihydroindenofluorenyl core ($d_{C/plane} \approx 3.3$ Å, $d_{H/plane} \approx 2.5$ Å). This ring bridging will have remarkable electronic consequences.

We investigated the electrochemical behavior of **1** and **2** by cyclic voltammetry. Two successive oxidation waves were observed, with maxima at 1.53 and 1.94 V for **1** and at 1.57 and 1.88 V for **2** (versus the saturated calomel electrode; see the Supporting Information). The first monoelectronic oxidation wave was assigned for both compounds to the oxidation of the dihydroindenofluorenyl core, and the second multielectronic wave surely involves the concomitant oxidation of the

fluorenyl units and the dihydroindenofluorenyl radical cation. Two important features and their consequences on the oxidation need to be stressed: 1) the *meta*-linkage effect and 2) the ring-bridging effect. Indeed, the first oxidation potentials for both **1** and **2** are more positive than those of their isomers **6** and **7** (1.36 and 1.43 V, respectively).[14,25] As the first electron transfer is centered on the dihydroindenofluorenyl core for the four isomers, this anodic shift may be directly related to the *para* or *meta* linkages and is hence clearly indicative of a shorter π-conjugation pathway in **1** and **2**. Secondly, there is also a slight shift in the first oxidation potential between **1** (1.53 V) and **2** (1.57 V), despite their identical *meta* linkages. This small potential difference was assigned to the contraction of the dihydroindeno[1,2-*a*]fluorenyl core (versus the (2,1-*b*) core) as a result of the presence of a spiro bridge *ortho* to both phenyl linkages. This contraction leads to a deformation of the dihydroindeno-[1,2-*a*]fluorenyl core (as observed in the crystallographic structure of **2**; Figure 1, right), which induces a poorer delocalization of π-electrons and hence a more anodic first oxidation potential. These features highlight the importance of the ring bridging and its influence on the π conjugation.[26] Thus, both **1** and **2** possess wide HOMO/LUMO differences: $\Delta E_{El} = 4.05/4.16$ eV, respectively, with HOMO/LUMO levels lying at −5.80/−1.75 eV for **1** and at −5.86/−1.70 eV for **2** (as evaluated from the onset oxidation/reduction potentials; see the Supporting Information). Geometry optimizations of **1** and **2** in the singlet state were also performed by density functional theory (DFT) at the Gaussian09 B3LYP/6-311 + G** level of theory. Despite a slight deviation, the calculated HOMO/LUMO energy differences ($\Delta E_{cal} = 4.36$ eV, HOMO/LUMO: −5.73/−1.37 eV for **1** and $\Delta E_{cal} = 4.42$ eV, HOMO/LUMO: −5.80/−1.38 eV for **2**; see the Supporting Information) are fully consistent with the electrochemical data.

The UV/Vis absorption spectrum of **1** (in THF) exhibits five characteristic bands (298, 310, 326, 334, and 342 nm; Figure 2a) that are very similar to those previously observed for its *para* homologue **7**, but with a slight blue shift of 2/3 nm, which suggests, as explained above, a poorer delocalization of π-electrons owing to the different linkages (*para* versus *meta*).

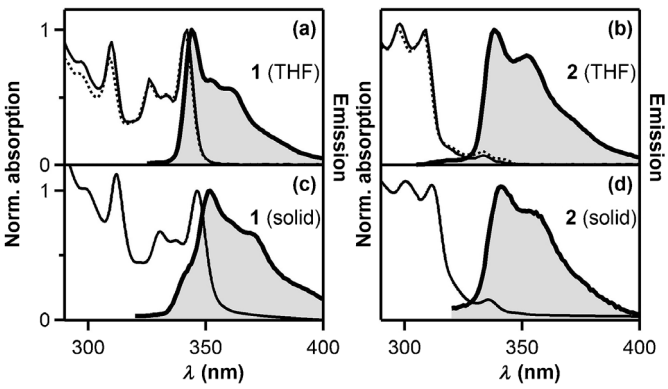

Figure 2. Absorption (thin solid lines), fluorescence (bold solid lines), and excitation spectra (dotted lines) of **1** (left) and **2** (right) in THF (a,b) and as thin films (c,d). Emission spectra: $\lambda_{exc} = 300$ nm (solution in THF) or 310 nm (thin film). Excitation spectra: $\lambda_{em} = 355$ nm.

The emission spectrum of **1** is well-resolved with a main band at 344 nm and with a very small Stokes shift of 2 nm, indicative of little nuclear rearrangement in the excited state and hence a very rigid structure. This feature should be linked to the high quantum yield of approximately 0.54, making this compound an efficient violet emitter. Moreover, the excitation spectrum of **1** overlaps quite well with the absorption spectrum. The fluorescence decay curves of **1** in THF under both 300 and 330 nm laser excitation (see Figure S5 in the Supporting Information) provides a single lifetime of 3.95 ns, which is noticeably longer than the corresponding lifetimes of its *para* analogues **6** (2.08 ns) and **7** (1.95 ns).[27] The radiative rate constant (k_r) of **1** was calculated to be $1.4 \times 10^8\ s^{-1}$, which is about half the value of k_r of **6** and **7** (2.9×10^8 and $3.2 \times 10^8\ s^{-1}$, respectively). The same conclusion was drawn for the nonradiative rate constant (k_{nr}) of **1** ($k_{nr} = 1.2 \times 10^8\ s^{-1}$), which represents 60% of the corresponding value for the *para* homologues ($k_{nr} = 1.9 \times 10^8\ s^{-1}$ for both **6** and **7**)[27] and thus confirms the structural rigidity of **1**.

However, the UV/Vis absorption spectrum of **2** (Figure 2b) has a drastically and surprisingly different shape to that of its isomer **1**; this difference clearly highlights the importance of the ring bridging. Indeed, the spectrum of **2** possesses three main bands: two intense bands at 298/309 nm and a very weak band at 333 nm followed by a shoulder at 342 nm. The molar absorption coefficient corresponding to the band at 333 nm is 18 times lower than that observed for its isomer **1** (**1**: $\varepsilon_{342nm} = 1.8 \times 10^4\ L\,mol^{-1}\,cm^{-1}$, **2:** $\varepsilon_{333nm} = 0.1 \times 10^4\ L\,mol^{-1}\,cm^{-1}$). TD-DFT calculations performed at the Gaussian09 B3LYP/6-311 + G** level of theory reveal that the lowest calculated energy transitions of **1** and **2**, corresponding to a π–π* transition located on the dihydroindenofluorenyl core, have oscillator strengths of approximately 0.24 and 0.02, respectively (see the Supporting Information). These values are in good agreement with the molar absorption coefficients obtained experimentally for these transitions. Thus, the extremely weak band recorded for **2** at 333 nm seems to be a unique feature of dihydroindenofluorene derivatives. Indeed, the (2,1-*b*), (1,2-*b*), and (2,1-*a*) isomers (and more generally oligophenylene derivatives) all exhibit high molar absorption coefficients (**6**: $\varepsilon_{339nm} = 3.08 \times 10^4\ L\,mol^{-1}\,cm^{-1}$, **7**: $\varepsilon_{344nm} = 3.23 \times 10^4\ L\,mol^{-1}\,cm^{-1}$ in THF). This peculiar behavior of **2** may be related to symmetry considerations. Unlike its (2,1-*b*), (1,2-*b*), and (2,1-*a*) congeners, **2** has no symmetry axis or symmetry plane, and its constrained structure leads to a clear deformation of the dihydroindeno[1,2-*a*]fluorenyl core, with off-plane dihedral angles as described above (Figure 1). Such structural features seem to have a strong influence on the character of the partially allowed/forbidden character of the first π–π* transition of **2** (see TDDFT calculations of **1**, **2**, **6**, and **7** in the Supporting Information).

The fluorescence spectrum of **2** is hypsochromically shifted (6 nm) relative to that of its isomer **1**; this shift again highlights the effect of the ring bridging on the π-conjugation. The quantum yield of **2** is also surprisingly recorded at 0.23, twice smaller than that of **1** and of *para* analogues **6** and **7**.[14] Surprisingly, the fluorescence decay of **2** (in THF) upon excitation at 300 nm (see Figure S5) showed two components:

a major time constant $\tau_1 = 9.04$ ns with a preexponential factor of 90%, and a minor time constant $\tau_2 = 2.73$ ns, which represents only 10% of the decay. Interestingly, the fluorescence decay curve recorded under excitation at 330 nm can be analyzed with the same τ_1 and τ_2 time constants, but with inverted proportions (42% for τ_1 and 58% for τ_2). The calculation of radiative and nonradiative rate constants of **2**, based on an average lifetime $\langle\tau\rangle = 8.0$ ns,[28] provides $k_r = 2.9 \times 10^7\ s^{-1}$, which is much lower than **1**, and $k_{nr} = 1.0 \times 10^8\ s^{-1}$, which is comparable to that of **1**. Thus, the loss of fluorescence quantum yield in the case of **2** mainly results in its much lower electronic transition moment, but not in more efficient internal conversion processes. Such intriguing and unusual emission properties may be the signature of unconventional processes, such as the presence of several emissive states in compound **2**, or partially decoupled excited states, or even different molecular conformers of **2**.

All-in-all, these preliminary results clearly stressed the unique photophysical properties of the dihydroindeno[1,2-*a*]fluorenyl backbone as compared to other dihydroindenofluorenes previously reported and more generally to π-conjugated oligophenylenes. If it is clear that the ring bridging is at the origin of this spectacular effect, more detailed theoretical and spectroscopic investigations need to be conducted to fully unravel this critical issue. UV/Vis absorption and fluorescence spectra of **1** and **2** in the solid state as spin-coated thin films appeared to be similar to the respective solution spectra, but with a slight red shift of less than 10 nm due to the different dielectric constants of the environment (Figure 2c,d). This similarity between the solid-state and solution spectra indicates weak π–π intermolecular interactions in the solid state and hence isolated fluorophores. As the stability of the emission is a key point for any OLED applications, spin-coated thin films of **1** and **2** were exposed to air under thermal stress conditions in an accelerated lifetime test (see the Supporting Information). As no low-energy emission bands beyond 400 nm were detected, the emission color of **1** and **2** appears to be stable (owing to steric protection by the spirofluorene units), which is a promising feature for the stability of the OLED emission (see below).

Finally, to examine the potential application of these new fluorophores, we investigated nondoped SMOLEDs with either **1** (device 1) or **2** (device 2) as the EML (see device architecture in the Supporting Information). The normalized electroluminescence (EL) spectra for both devices are very similar, with a main peak around 390–400 nm (see Figure S24) corresponding to a blue light with CIE color coordinates (Table 1) close to the NTSC standard for blue (0.14, 0.08). The turn-on voltage appears to be low for a blue device (V_{on} = 4.5 V for device 1 and 4.9 V for device 2) and thus indicates an efficient charge injection. Device 1 is more efficient than device 2, with a maximum current efficiency (CE) of 0.7 cd A^{-1} (0.4 cd A^{-1} for device 2) and an external quantum efficiency (EQE) of 0.9% (0.5% for device 2; Table 1). This result may be explained by the slightly more violet emission of device 2 as compared to device 1, as it is known that the EL efficiency is always lower when the color of the OLED is shifted towards the violet. However, the different quantum yields of **2** and **1** (0.23 versus 0.54) may also be the reason for different device efficiency. Despite the simple chemical design of the fluorophores **1** and **2**, the performance of the OLED with **1** as the EML is, to the best of our knowledge, around the highest reported for indenofluorene-based nondoped blue OLEDs;[5–8] this result points out the high potential of these new dihydroindenofluorenyl moieties. The use of electron-/hole-transporting moieties attached to the fluorene or to the dihydroindenofluorene cores, a well-known and efficient strategy, will allow further improvement of the performance of the devices.

Table 1: EL characteristics of devices 1 and 2.

Device	V_{on}[a] [V]	EQE[b] [%]	CE[b] [cd A^{-1}]	Lum.[c] [cd m^{-2}]	CIE	
					x	*y*
1	4.5	0.9	0.7	704	0.201	0.188
2	4.9	0.5	0.4	200	0.193	0.128

[a] Value for a luminance of 0.1 cd m^{-2}. [b] Value for a current efficiency of 10 mA cm^{-2}. [c] Maximum luminance.

To summarize, we have synthesized two new dihydroindeno[1,2-*a*]fluorenyl and dihydroindeno[2,1-*b*]fluorenyl positional isomers (**1** and **2**, respectively) and established an efficient synthetic approach that enables both isomers to be obtained simultaneously. A remarkable effect of positional isomerism on spectroscopic properties was found for the (1,2-*a*) isomer **2**, thus highlighting the importance of the ring bridging in oligophenylene chemistry. Finally, **1** and **2** were successfully employed as the EML in nondoped blue OLEDs with performance close to the highest reported for dihydroindenofluorene-based OLEDs. This study, which to the best of our knowledge appears to be the first example of the incorporation of dihydroindeno[1,2-*a*]fluorenyl and dihydroindeno[2,1-*b*]fluorenyl cores in nondoped blue OLEDs, highlights the potential of these new organic semiconductors. As the development of organic electronics is driven by the synthesis of new molecular fragments, we believe that dihydroindeno[1,2-*a*]fluorene and dihydroindeno[2,1-*b*]fluorene families could play a key role in the future.

Received: July 30, 2013
Revised: September 20, 2013
Published online: November 7, 2013

Keywords: blue emission · dihydroindenofluorene isomers · light-emitting diodes · organic semiconductors · ring bridging

[1] Thematic issue: π-Functional Materials; special-issue editors: J. L. Bredas, S. R. Marder, E. Reichmanis, *Chem. Mater.* **2011**, *23*, 309 – 922.
[2] A. C. Grimsdale, K. Müllen, *Macromol. Rapid Commun.* **2007**, *28*, 1676 – 1702.
[3] A. C. Grimsdale, K. L. Chan, R. E. Martin, P. G. Jokisz, A. B. Holmes, *Chem. Rev.* **2009**, *109*, 897 – 1091.
[4] W. Deuschel, *Helv. Chim. Acta* **1951**, *34*, 2403 – 2416.
[5] J. Jacob, J. Zhang, A. C. Grimsdale, K. Müllen, M. Gaal, E. J. W. List, *Macromolecules* **2003**, *36*, 8240 – 8245.
[6] Y. Park, J.-H. Lee, D. H. Jung, S.-H. Liu, Y.-H. Lin, L.-Y. Chen, C.-C. Wu, J. Park, *J. Mater. Chem.* **2010**, *20*, 5930 – 5936.

[7] D. Thirion, J. Rault-Berthelot, L. Vignau, C. Poriel, *Org. Lett.* **2011**, *13*, 4418 – 4421.
[8] D. Marsitzky, J. C. Scott, J.-P. Chen, V. Y. Lee, R. D. Miller, S. Setayesh, K. Müllen, *Adv. Mater.* **2001**, *13*, 1096 – 1099.
[9] L.-C. Chi, W.-Y. Hung, H.-C. Chiu, K.-T. Wong, *Chem. Commun.* **2009**, 3892 – 3894.
[10] W. Zhang, J. Smith, R. Hamilton, M. Heeney, J. Kirkpatrick, K. Song, S. E. Watkins, T. Anthopoulos, I. McCulloch, *J. Am. Chem. Soc.* **2009**, *131*, 10814 – 10815.
[11] H. Usta, C. Risko, Z. Wang, H. Huang, M. K. Deliomeroglu, A. Zhukhovitskiy, A. Facchetti, T. J. Marks, *J. Am. Chem. Soc.* **2009**, *131*, 5586 – 5608.
[12] D. T. Chase, A. G. Fix, S. J. Kang, B. D. Rose, C. Weber, Y. Zhong, L. Zakharov, M. C. Lonergan, C. Nuckolls, M. M. Haley, *J. Am. Chem. Soc.* **2012**, *134*, 10349 – 10352.
[13] Q. Zheng, B. J. Jung, J. Sun, H. E. Katz, *J. Am. Chem. Soc.* **2010**, *132*, 5394 – 5404.
[14] D. Thirion, C. Poriel, J. Rault-Berthelot, F. Barrière, O. Jeannin, *Chem. Eur. J.* **2010**, *16*, 13646 – 13658.
[15] D. Thirion, M. Romain, J. Rault-Berthelot, C. Poriel, *J. Mater. Chem.* **2012**, *22*, 7149 – 7157.
[16] J.-I. Nishida, S. Tsukaguchi, Y. Yamashita, *Chem. Eur. J.* **2012**, *18*, 8964 – 8970.
[17] A. Shimizu, R. Kishi, M. Nakano, D. Shiomi, K. Sato, T. Takui, I. Hisaki, M. Miyata, Y. Tobe, *Angew. Chem.* **2013**, *125*, 6192 – 6195; *Angew. Chem. Int. Ed.* **2013**, *52*, 6076 – 6079.
[18] D. T. Chase, B. D. Rose, S. P. Mc Clintock, L. N. Zakharov, M. M. Haley, *Angew. Chem.* **2011**, *123*, 1159 – 1162; *Angew. Chem. Int. Ed.* **2011**, *50*, 1127 – 1130.
[19] A. Shimizu, Y. Tobe, *Angew. Chem.* **2011**, *123*, 7038 – 7042; *Angew. Chem. Int. Ed.* **2011**, *50*, 6906 – 6910.
[20] A. G. Fix, P. E. Deal, C. L. Vonnegut, B. D. Rose, L. N. Zakharov, M. M. Haley, *Org. Lett.* **2013**, *15*, 1362 – 1365.
[21] L. Chardonnens, R. Ritter, *Helv. Chim. Acta* **1955**, *38*, 393 – 396.
[22] C. Poriel, R. Métivier, J. Rault-Berthelot, D. Thirion, F. Barrière, O. Jeannin, *Chem. Commun.* **2011**, *47*, 11703 – 11705.
[23] T. Kowada, S. Yamaguchi, K. Ohe, *Org. Lett.* **2010**, *12*, 296 – 299.
[24] C. Poriel, J. Rault-Berthelot, F. Barrière, A. M. Z. Slawin, *Org. Lett.* **2008**, *10*, 373 – 376.
[25] C. Poriel, J. Rault-Berthelot, D. Thirion, *J. Org. Chem.* **2013**, *78*, 886 – 898.
[26] H.-H. Huang, C. Prabhakar, K.-C. Tang, P.-T. Chou, G.-J. Huang, J.-S. Yang, *J. Am. Chem. Soc.* **2011**, *133*, 8028 – 8039.
[27] D. Thirion, C. Poriel, R. Métivier, J. Rault-Berthelot, F. Barrière, O. Jeannin, *Chem. Eur. J.* **2011**, *17*, 10272 – 10287.
[28] The average lifetime was calculated as:

$$\langle\tau\rangle = \frac{a_1\times\tau_1^2+a_2\times\tau_2^2}{a_1\times\tau_1+a_2\times\tau_2}.$$

A mean value of $\langle\tau\rangle$ of 8.0 ns was found for laser excitation at 300 and 330 nm.

